

## Hard X-Ray Diffraction Microscopy at SPring-8

Yoshinori Nishino<sup>1,\*</sup>, Jianwei Miao<sup>2</sup>, Yoshiaki Kohmura<sup>1</sup>, Yukio Takahashi<sup>1</sup>, Changyong Song<sup>2</sup>,  
Bart Johnson<sup>3</sup>, Masaki Yamamoto<sup>1</sup>, Kuniaki Koike<sup>4</sup>, Toshikazu Ebisuzaki<sup>4</sup> and Tetsuya Ishikawa<sup>1</sup>

<sup>1</sup>SPring-8/RIKEN, 1-1-1 Kouto, Mikazuki, Sayo, Hyogo, 679-5148, Japan

<sup>2</sup>Department of Physics and Astronomy and California Nanosystems Institute, University of California, Los Angeles,  
California 90095-1547, USA

<sup>3</sup>Stanford Synchrotron Radiation Laboratory, Stanford Linear Accelerator Center, Stanford, California 94309-0210,  
USA

<sup>4</sup>RIKEN, 2-1 Hirosawa, Wako, Saitama, 351-0198, Japan

We review the development of hard x-ray diffraction microscopy at SPring-8. We describe two approaches to enable image reconstruction solely from the diffraction intensity data: One is the iterative normalization algorithm, and the other is to experimentally confine the missing data region within the centro-speckle. In the both approaches, we obtained successful reconstruction in experiment as well as in simulation. Also, we report recent development of a computer system for serial image reconstruction during experiment, and a large-area in-vacuum imaging plate detector with the objective of achieving higher spatial resolution.

**KEYWORDS:** X-ray Diffraction Microscopy, Oversampling Phasing Method, Coherent X-rays, Hard X-rays

### 1. Introduction

X-ray diffraction microscopy is an innovative method to reconstruct high-spatial-resolution images from oversampled Fraunhofer diffraction intensities of non-crystalline samples. As the ultimate spatial resolution is limited by the x-ray wavelength, shorter-wavelength hard x-rays are beneficial to achieve higher resolution. Using hard-x-ray beamline BL29XUL at SPring-8, we have been developing x-ray diffraction microscopes.

At the initial stage of our study, we measured artificial patterns made by electron lithography. In ref. 1, we reported the measurement of nickel patterns on two layers; one is on the top surface and the other in 1  $\mu\text{m}$  depth. Though only the pattern on the top surface was imaged with scanning electron microscopy (SEM), two-dimensional x-ray diffraction microscopy provided an overlapped image of the two layers due to the high penetration depth of x-rays. A three-dimensional image of the sample was also obtained by using diffraction data at a number of incident angles. The highest spatial resolution in two-dimensional reconstruction, which we obtained using an artificial pattern, was 7 nm<sup>2</sup>) and the single pixel size of the reconstructed image was 3.5 nm.

Following the success with artificial pattern samples, we have been pursuing application works. In biological application, we measured Escherichia coli bacteria labeled with KMnO<sub>4</sub><sup>3</sup>). In materials science, porous silica particles were measured<sup>4</sup>). In the latter example, we reconstructed the absolute values of the sample electron density distribution by normalizing the diffraction intensities by the incident intensity. These examples illustrate the potential impact of x-ray diffraction microscope in these and other scientific fields.

### 2. Missing Near-Forward Diffraction Data Problem

In experiments of x-ray diffraction microscopy, near-forward diffraction intensity data are always missing: In the exact forward pixel, the additional transmitted x-rays make it impossible to extract the forward diffraction intensity; and near-forward diffraction intensities are difficult to measure due to parasitic scatterings from optical components, such as a pinhole and a guard slit. Also, because of the limited dy-

namic range of an area detector, a beamstop has to be placed in front of the detector to block intolerably intense diffracted x-rays in near-forward direction.

Although near-forward diffraction intensity data are missing in experiment, they contain important information: The exact-forward diffraction intensity determines the total number of electrons in the sample; and the near-forward data correspond to low spatial frequency modes of the sample and determine the approximate shape of the sample.

Because of the importance of the information in the missing data, it has not been possible, until recently, to reconstruct a sample image solely from the x-ray diffraction data. In our early experiments, the Fourier transform of a low-resolution sample image taken by soft x-ray microscope was

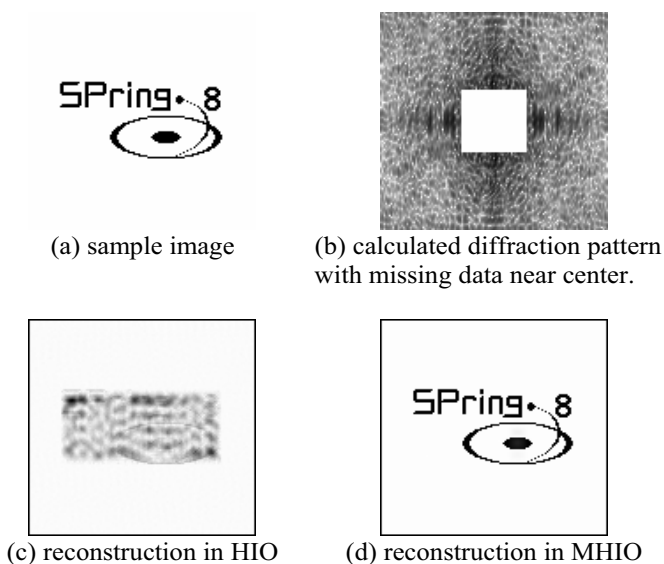


Fig. 1 simulation of image reconstruction with the HIO and MHIO algorithms<sup>5</sup>). In the calculated diffraction pattern (b), data at central 37 $\times$ 37 pixels are missing out of the total 129 $\times$ 129 pixels.

\* e-mail address: nishino@spring8.or.jp

used to complement the missing data. In order to solve this missing near-forward diffraction data problem, we developed two approaches, one in data analysis and the other in experiment.

### 2.1 Iterative normalization algorithm

In image reconstruction from oversampled Fraunhofer diffraction intensities, the HIO (hybrid input-output) algorithm proposed by Finup is widely used. In the HIO algorithm, the Fourier transform of an estimated sample electron density distribution and its inverse Fourier transform are iteratively performed with applying constraints at each iteration in the both reciprocal-space and real-space domain. In the reciprocal-space domain, measured values of the diffraction intensities are supplied; and in the real-space domain the support and positivity constraints are applied to the sample electron density distribution. The algorithm shows excellent convergence when there are no missing data. But our simulation showed that with large missing near-forward diffraction data, the estimated total number of electrons in the sample increased with iteration, and reconstruction failed as shown in fig. 1. This can be understood from the fact that the HIO algorithm proceeds to enhance the ratio of the numbers of electrons inside and outside the support. Without near-forward data, the total number of electrons is not fixed, and therefore the number of electrons in the support increases uncontrollably.

In order to overcome this difficulty, we developed a new image reconstruction algorithm named MHIO (modified HIO) algorithm, where the total number of electrons is iteratively normalized without the knowledge of the true total number of electrons<sup>5)</sup>. Simulation in fig. 1 shows successful reconstruction in the MHIO algorithm from the diffraction data with largely missing near-forward diffraction data.

The algorithm was also successfully applied to experimental data of a gold pattern sample. The diffraction data were measured at a x-ray wavelength of 2.13 Å using BL29XU at SPring-8. While image reconstruction was not successful

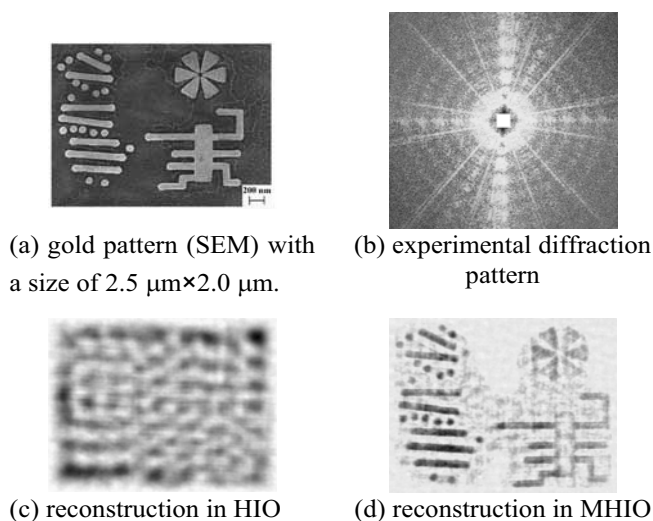


Fig. 2 image reconstruction from experimental diffraction data with the HIO and MHIO algorithms<sup>5)</sup>. In the experimental diffraction pattern (b), data at central 61×61 pixels are missing out of the total 1001×1001 pixels. The single pixel size of the reconstructed images, (c) and (d), is 7 nm square.

with the conventional HIO algorithm, a remarkable improvement was observed with the MHIO algorithm as shown in Fig 2. The result demonstrates the effectiveness of the iterative normalization of the MHIO algorithm.

### 2.2 Missing diffraction data within centro-speckle

In addition to the development of the image reconstruction algorithm, we made efforts to reduce the area of missing data. When the missing data region is confined within the centro-speckle, missing information is considerably reduced. To this end, we made modifications to the experimental setup. The modifications include using a silicon window frame with tapered edges for a guard slit; placing a beamstop very close to a CCD (charge-coupled device) detector; and increasing the sample-to-detector distance to 1120 mm. The increase of the sample-to-detector distance makes the oversampling ratio and thus the speckle size larger, though it is accompanied by the deterioration of the spatial resolution of the reconstructed image.

Fig. 3 shows an experimental result with the modified setup<sup>6)</sup>. The experiment was performed using GaN particles as samples at BL29XU in SPring-8. X-rays with a wavelength of 2.48 Å were used to record the diffraction data. We successfully reconstructed the sample image from the diffraction data alone, as shown in Fig. 3 (c), by using the HIO algorithm.

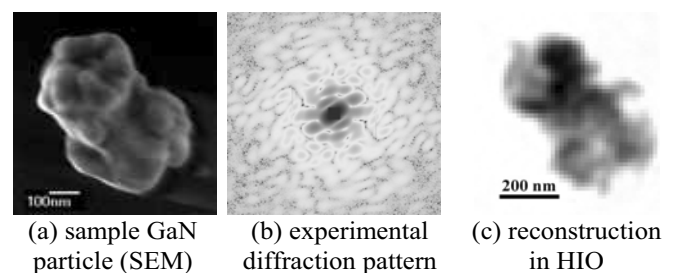


Fig. 3 image reconstruction from experimental diffraction data with missing data within the centro-speckle<sup>6)</sup>. In the experimental diffraction pattern (b), the missing data region was confined within the centro-speckle and had a size of 29 × 29 pixels. The single pixel size of the reconstructed image (c) is 15 nm square.

## 3. Dynamic Reconfigurable Processors for Image reconstruction

Reconstruction of a sample image solely from the x-ray diffraction data became possible with approaches, proposed by our group and other groups, to the problem of missing near-forward diffraction data, as shown in the previous section. These developments have considerable significance in applications of the microscope. For example, it enables studies on sample dynamics; it also promotes analysis of biological samples, where radiation damage poses a serious problem. In both examples of application, a low resolution image of a sample is difficult to measure after the x-ray diffraction measurement. Also from an experimental point of view, it offers an advantage that one can get quick feedback from the measurement by serially reconstructing sample images immediately after the diffraction measurement.

In order to make image reconstruction faster in parallel with measurement, we are developing a computer system using dynamic reconfigurable processors in collaboration

with IP FLEX Inc <sup>7)</sup>. The hardware configuration of a dynamic reconfigurable processor can be optimized for a specific application as in ASIC (application specific integration circuit), but unlike ASIC the configuration can be change dynamically in one clock cycle. In the present case of 166 MHz clock frequency, the reconfiguration takes only about 6 ns.

In image reconstruction with dynamic reconfigurable processors, computation tasks at each iteration are divided into four steps: fast Fourier transform (FFT), the reciprocal space constraint, inverse FFT, and the real space constraint. The processors change configuration to optimize themselves for each of the four steps. For example, the processor optimized for FFT can perform the operation about 13 times faster than 3.60 GHz Intel Pentium 4 Processor. As for image reconstruction, it executes 1000 iterations of a  $1024 \times 1024$  pixel image in 87 s.

#### 4. Large-Area In-Vacuum Imaging Plate Detector

In our studies of x-ray diffraction microscopy, short wavelength hard x-rays have been used to achieve high spatial resolution. With x-rays of a specific wavelength, the best resolution attainable in experiment is determined by the highest diffraction angle of recorded diffraction data, if radiation damage of the sample can be neglected. In previous experiments we have been using a CCD detector with a total area of about one inch square. The best spatial resolution of 7 nm in ref. 2 was obtained by combining diffraction data at different CCD positions to cover up to a large diffraction angle.

To attain even higher spatial resolution we are developing an in-vacuum imaging plate detector in collaboration with RIGAKU <sup>8)</sup>. A picture of the detector is shown in fig. 4. Unlike other x-ray area detectors, large area is easily commercially available with imaging plates, and an imaging plate of the detector has a total area of 125 mm square. Also, a small pixel size is required in order to satisfy the oversampling condition with a moderate sample-to-detector distance. With a small pixel size of 25  $\mu\text{m}$  and a large total detector area, a  $5000 \times 5000$  pixel array is achieved.

Imaging plates also feature a wide dynamic range of  $10^4$  or higher (two orders of magnitude greater than that of our direct illumination CCD detector).

A drawback of imaging plates is slow in reading and erasing. With the detector under development, it takes about five

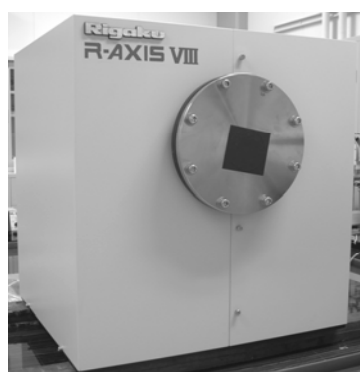


Fig. 4 in-vacuum imaging plate detector R-AXIS VIII developed in collaboration with RIGAKU.

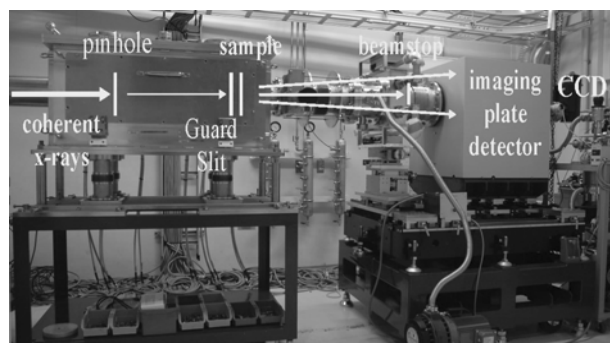


Fig. 5 planned experimental setup with the in-vacuum imaging plate detector.

minutes for reading and about one minute for erasing. To perform effective measurement with imaging plates, the detector has two sets of imaging plate, reader and eraser, and one can record data with one imaging plate while reading or erasing the other.

Because diffraction intensities are weak for non-crystalline samples especially at high diffraction angles, the whole experimental setup including the sample and the imaging plates are placed in a vacuum in order to avoid unwanted air scattering, while the reader and eraser are in the air. Reading and erasing of imaging plates are conducted through pressure-proof glasses. Fig. 5 shows a picture of a planned experimental setup.

#### 5. Summary

Activities of x-ray diffraction microscopy at SPring-8 were reviewed. In early experiments we have succeeded in image reconstruction of samples in biology and materials science. In these works, a supplemental low resolution image of the sample was necessary due to the problem of missing near-forward diffraction data. In order to enable direct image reconstruction solely from x-ray diffraction data, we developed two approaches. One is the MHIO algorithm, where the number of electrons is iteratively normalized. And the other is to experimentally confine the missing data region within the centro-speckle and thus to reduce the missing information. With these developments it became experimentally possible to reconstruct a sample image from the x-ray diffraction data alone. It made also possible to serially reconstruct sample images immediately after diffraction measurement. To perform fast image reconstruction during experiment, we are developing a computer system using dynamic reconfigurable processors. We are also developing an in-vacuum imaging plate detector to achieve higher spatial resolution. The detector has a total size of 125 mm square and a pixel size of 25  $\mu\text{m}$ .

- 1) J. Miao, T. Ishikawa, B. Johnson, E. H. Anderson, B. Lai and K. O. Hodgson: Phys. Rev. Lett. **89** (2002) 088303.
- 2) J. Miao, T. Ishikawa, E. H. Anderson and K. O. Hodgson: Phys. Rev. B **67** (2003) 174104.
- 3) J. Miao, K. O. Hodgson, T. Ishikawa, C. A. Larabell, M. A. LeGros and Y. Nishino: Proc. Natl. Acad. Sci. USA **100** (2003) 110.
- 4) J. Miao, J. E. Amonette, Y. Nishino, T. Ishikawa and K. O. Hodgson: Phys. Rev. B **68** (2003) 012201.
- 5) Y. Nishino, J. Miao and T. Ishikawa: Phys. Rev. B **68** (2003) 220101(R).
- 6) J. Miao, Y. Nishino, Y. Kohmura, B. Johnson, C. Song, S. H. Risbud and T. Ishikawa: Phys. Rev. Lett. in press (2005).
- 7) IP FLEX Inc. (<http://www.ipflex.com/>).
- 8) RIGAKU (<http://www.rigaku.co.jp/>).